



# Mechanistic study of drag reduction in turbulent pipeline flow over anionic polymer and surfactant mixtures

Yanlin Chai<sup>1</sup> · Xianwen Li<sup>2</sup> · Jiafeng Geng<sup>1</sup> · Jiaxin Pan<sup>1</sup> · Yalong Huang<sup>1</sup> · Dengwei Jing<sup>1</sup>

Received: 24 April 2019 / Revised: 23 May 2019 / Accepted: 11 June 2019 / Published online: 27 June 2019  
© Springer-Verlag GmbH Germany, part of Springer Nature 2019

## Abstract

The mixed aqueous solutions of anionic surfactant sodium dodecyl sulfate with polymer polyacrylamide of various kinds, i.e., cationic, anionic, nonionic, and zwitterion, were firstly tested to study their synergistic effect on drag reduction performance. The optimal combination of sodium dodecyl sulfate with anionic polyacrylamide was confirmed due to their strong hydrophobic interaction and electrostatic repulsion caused by the same charge. The surface tension, conductivity, and viscosity of pure surfactant solution and mixed solutions at different surfactant concentrations with anionic polymer of certain concentration were tested, and their drag reduction behavior in pipe flow was also investigated experimentally. It turns out that drag reduction performance acquired from the combination of anionic surfactant and anionic polyacrylamide is better than either of the single additive, especially under high shear rate. For the mixtures, the degree of drag reduction is strongly dependent on the concentration of SDS and more pronounced in the high Reynolds number range. The best drag reduction performance is obtained for the SDS concentration around the polymer saturation point. Our work should be of value for the drag reduction in the application such as shale gas fracturing and various fluid transports.

**Keywords** Drag reduction · Anionic surfactant · Anionic polymer · Surface tension · Conductivity · Viscosity

## Introduction

Drag reduction is a phenomenon that exhibits a lower pressure drop for the same flow rate in the pipe flow [1]. It is well known that the presence of small amounts of certain additives (drag reducer) in water can result in a considerable reduction of drag in turbulent flow, which can reduce pumping power and increase piping system capacity [2, 3]. Such areas of interest where these additives are particularly gaining tremendous attention are oil production [4], district heating and cooling [5, 6], sewage systems [7], and firefighting [8].

The additives causing drag reduction can be divided into five categories: polymers, surfactants, fibers, microbubbles, and compliant coating [9]. Surfactants and polymers are most

commonly used in industrial application. The drag reduction ability of polymers depends on many factors such as molecular weight, aggregation, and chain flexibility [10, 11]. In general, the most effective drag-reducing polymers possess a linear flexible structure and high molecular weight. As a usual drag reducer, polyacrylamide (PAM) has often been used; in some cases, surfactants were also employed. The drag reduction capability of surfactant is primarily affected by its concentration and the ability to form a wormlike micelle. Typical examples of the used surfactants for drag reduction is anionic surfactant sodium lauryl sulfate (SDS) and cationic surfactant cetyltrimethylammonium chloride (CTAC) [12]. In fact, both polymers and surfactants have certain advantages over each other when used as drag reducer. For example, polymers become effective at very low concentrations whereas surfactants become effective only at concentrations well above the critical micelle concentration (CMC). Moreover, the drag reduction capabilities of surfactants are affected by temperature due to the strong temperature dependence of micelle formation. However, the greatest advantage of surfactants is that the shear-induced structures in these systems are of regenerative nature whereas the polymer macromolecules undergo permanent mechanical breakdown under high shear stress

✉ Dengwei Jing  
dwjing@xjtu.edu.cn

<sup>1</sup> State Key Laboratory of Multiphase Flow in Power Engineering & International Research Center for Renewable Energy, Xi'an Jiaotong University, Xi'an 710049, China

<sup>2</sup> Oil and Gas Technology Research Institute of Changqing Oilfield Company, Xi'an 710018, China

conditions. Thus, surfactants are preferred over polymers in applications involving cyclic high shear–stress conditions [13].

Studies have shown that the association of water-soluble polymer and surfactant can retain the advantages of a variety of original single materials, making up for its shortcomings, improving drag reduction efficiency, and enhancing drag stability for the formation of complexes or aggregates of polymer and surfactant [14, 15]. It is well-known that the self-assembly of surfactant monomers occurs at CMC, whereas the interaction between polymers and surfactants begins at a different surfactant concentration called as the critical aggregation concentration (CAC). There are two types of interaction between polymers and surfactants: electrostatic interaction and hydrophobic interaction. Electrostatic interaction always exists in the polymer–surfactant system with charges. For the systems with no opposite charges, hydrophobic interaction could be the dominated one [16, 17]. When the interaction between the polymer and the surfactant is of the electrostatic type, namely, polymer and surfactant are both ionic with charges, and the CAC will be lower than the CMC. When the interaction is of the hydrophobic type (the hydrophobic parts of the nonionic polymer and ionic surfactant interact), the CAC is close to the CMC. Then, the interaction between polymers and surfactants will be saturated with the concentration of the surfactant increasing to the polymer saturation point (PSP) [18, 19]. The synergistic interactions between polymers and surfactants can dramatically alter the characteristics of the solution. The interactions depend upon several factors, such as the nature of the surfactant head group, the polar group embedded in the polymer backbone, polymer hydrophobicity, and flexibility [20].

Considerable efforts have been made to understand the interaction between different kinds of polymers and different types of surfactants. Among the investigations of synergistic interactions between polymers and surfactants, the most heavily reported is the combination of nonionic polymer and cationic surfactant. Liu [14, 21] et al. investigated the effect of mixed nonionic polyacrylamide and cationic surfactant CTAC solutions on drag reduction performance from the point of experiment and molecular dynamics simulation, respectively. The results prove that the viscosity of the CTAC/PAM/Nasal solution is significantly higher than that of the CTAC/Nasal solution for the surfactant micelles interacting with the polymer and form rod-like micelles, then the polymer–surfactant complex can intensify drag reduction at some extent, and temperatures were more influential than concentrations. Matras [22] et al. studied the influence of nonionic polymer polyoxyethylene (PEO) and CTAC aggregates on fluid flow and concluded that PEO–CTAB aggregates can reduce drag much more efficiently than these substances alone. Ali et al. [15, 23] investigated the effect of mixed PEO and cationic surfactant octadecyl trimethyl ammonium chloride (OTAC) solutions on drag reduction and their mechanical degradation.

The results indicated that the addition of surfactant to the polymer increases the extent of drag reduction range due to the formation of a new microstructure and improves the resistance of polymer chains against shear degradation, especially in solutions with low polymer concentration and high surfactant concentration. In addition, the effect of nonionic polymer PEO and anionic surfactant SDS on drag reduction behavior and mechanical degradation were also studied by Ali et al. [23, 24]. The relative viscosity showed a remarkable increase upon the addition of surfactant to the polymer solution due to extension of polymer chains caused by the formation of micelles on the backbone of the polymer molecules. The same authors also investigated the effect of anionic polymer PAM and cationic surfactant OTAC on drag reduction behavior and mechanical degradation [13, 23, 24]. The result suggested that the drag reduction capability of anionic polymer PAM is reduced upon the addition of oppositely charged cationic surfactant (OTAC) molecules due to charge neutralization and hence coiling of PAM chains. Also, the presence of surfactant accelerates mechanical degradation of polymer chains.

In order to explain the interaction between polymer and surfactants, some models have been proposed. One is the so-called necklace model proposed by Nagarajan [25]. For this model, a complex consisting of the polymer molecule wrapped around surfactant micelles is formed and the polymer segments partially penetrate into the polar head group region of the micelles, which causes a reduction in the micelle core and water contact area. For another Rosenstein model, a thermodynamic model based on the adsorption of polymer molecules onto the micelle surface has been proposed. The presence of polymer molecules in water changes the surface free energy between the micellar hydrocarbon core and the solvent in the “free space” of the coiled macromolecule [26].

In summary, the previous studies have shown that the more extended and stretched the polymer molecular chain is because of the interaction with the surfactant, the better drag reduction performance will be achieved. Accordingly, hydrophobic interaction and electrostatic repulsion can both facilitate the extension and stretch of the polymer molecular chain. Thus, it can be inferred that the polymer with the same charged surfactant may be extended more effectively for the stronger electrostatic repulsion interaction, then superior drag reduction behavior might be achieved. Unfortunately, to the best of our knowledge, there is no research on the interaction of polymer and surfactant with the same charge, nor the effect on drag reduction. The aim of this study is to select the optimum combination of anionic surfactant SDS, a kind of anionic surfactant with lower toxicity and smaller head group which is widely used in the industry, with different kinds of polymer PAM, to acquire the best drag reduction effect.

It is also expected to provide a better understanding of the interactions between SDS and same-charged PAM in aqueous solutions, to determine their effect on DR behavior in pipeline flow. Our work should be of value for the drag reduction in the application such as shale gas fracturing and various fluid transports.

## Materials and methods

### Materials

Four different kinds of polymer-polyacrylamide (PAM) (Gongyi Liqing Water Purification Material Factory), cationic PAM, anionic PAM, nonionic PAM, and zwitterion PAM with the molecular weight of  $M_v = 1.6 \times 10^7$ , were used in our investigation. Sodium dodecyl sulfate (SDS, purity  $\geq 99\%$ , Sinopharm Chemical Reagent Co. Ltd., China) was used as the anionic surfactant. Tap water (the conductivity of which is about  $216 \mu\text{S}/\text{cm}$ ) was utilized as the base fluid.

### Sample preparation

To prepare solutions containing polymer and surfactant, the surfactant and polymer were dissolved in tap water, respectively, and then mixed in the tank with the certain amount of tap water to acquire specific fluid. As a typical procedure, firstly, surfactant powders with the desired concentrations were dissolved in 1 L tap water. With the assistance of sufficient magnetic stirring, stable and clear surfactant solutions can be obtained. Meanwhile, 1 g PAM was added in 1 L tap water which is kept stationary for 12 h at room temperature firstly, then followed by fully stirring at 500 rpm/min for about 2 h at  $40 \pm 0.5 \text{ }^\circ\text{C}$  until it was dissolved and a homogenous polymer solution is obtained.

## Experimental setup and measurements

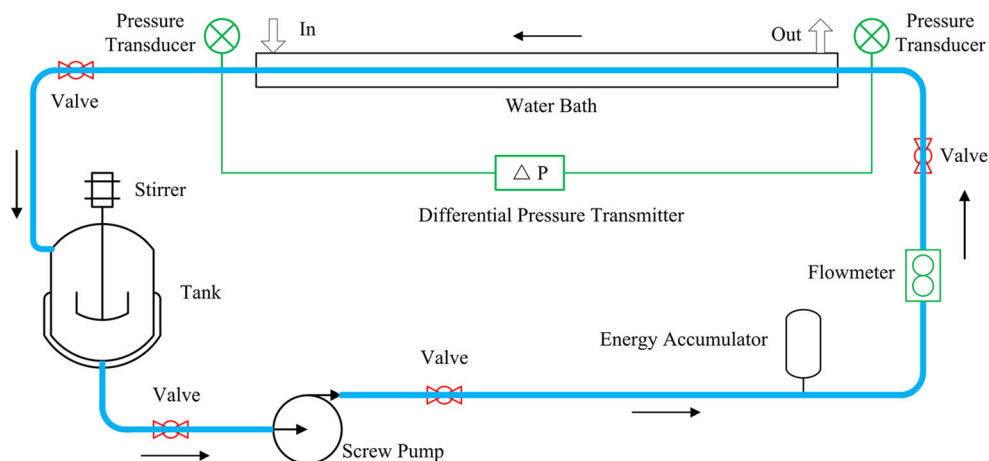
The pipeline experiments were carried out in a closed-loop system shown in Fig. 1. The test fluid was prepared in a large mixing tank which was circulated in a piping loop. The temperature inside the test section was maintained at  $20 \pm 0.5 \text{ }^\circ\text{C}$  by passing cold or hot water through the pipe jacket with the aid of a temperature controller. The external diameter of the test pipe is 10 mm with the wall thickness of 1 mm, and the total length of the pipeline is 10.8 m with the testing section being 3.3 m in length.

The fluid flow in the closed-loop system was driven by the stainless-steel screw pump, and the flow rates were adjusted from 0.2 to  $1.3 \text{ m}^3/\text{h}$  to ensure the output values of flow rate and pressure by an inverter to be relatively stable throughout the experiment. The pressure drop of the test section was measured by a differential pressure transmitter. The measuring accuracy of flow rate and pressure drop was  $0.01 \text{ m}^3/\text{h}$  and 0.1 kPa, respectively.

The temperature of the solution was maintained at  $20 \pm 0.5 \text{ }^\circ\text{C}$  by water bath, then the surface tension and conductivity were measured subsequently. A surface tension study was performed based on a contact angle meter (SL200B, Shanghai Zhongchen Digital Technology Apparatus Co. Ltd., China) by using the principle of drop shape tensiometer. In a nutshell, a droplet of the liquid sample was created at the tip of the syringe needle and a camera was equipped to capture the images. Based on the profile of the droplet, the surface tension value can be calculated by fitting the Young–Laplace equation [27].

Conductivity measurement was performed by Mettler desktop conductivity meter; every conductivity for the same sample was measured three times and took the average. Viscosity measurement was conducted by an Ubbelohde viscometer in an electro-thermostatic water cabinet to maintain the temperature to be  $20 \pm 0.5 \text{ }^\circ\text{C}$ . A chronograph was used to record the time for flowing through the measuring section of

**Fig. 1** Diagram of the experiment system



test fluid, and the densitometer to measure the density. Then, the viscosity would be acquired according to the corresponding formula.

## Data processing

In this work, the Reynolds number  $Re$  was determined as follows:

$$Re = \frac{ud\rho}{\mu}$$

where  $u$  is the bulk mean velocity,  $d$  is the diameter of the pipeline,  $\mu$  is the viscosity of solvent, and  $\rho$  is the density of the solvent.

The effectiveness of the drag-reducing surfactant polymer is determined by the percentage of drag reduction (DR) in a flowing fluid which is usually expressed quantitatively as follows:

$$DR\% = \frac{\Delta P_{\text{without additives}} - \Delta P_{\text{with additives}}}{\Delta P_{\text{without additives}}} \times 100\%$$

where  $\Delta P_{\text{without additives}}$  is the pressure drop in the absence of additives and  $\Delta P_{\text{with additives}}$  is the pressure drop in the presence of additives.

## Results and discussion

### Drag reduction effect of SDS with different kinds of PAM

Previous investigations have shown that the effect of the surfactant–polymer interaction on the drag reduction performance depends on the charge of surfactant and polymer simultaneously. Therefore, it is supposed that a kind of surfactant can demonstrate different drag reduction behavior when compounded with PAM of different charge. In our experiment, SDS is selected for its small size of the anionic head group and the hydrophobic conditions significantly contributing to the overall interaction with the polymer [23]. As mentioned, the interaction between polymers and surfactants begins at a different surfactant concentration (CAC) lower than the CMC, and the interaction is more obvious in solutions with low polymer concentration and high surfactant concentration [15, 18]. Here in our study, we chose the concentration of SDS to be 2000 ppm, which is around CMC, and the concentration of PAM relatively lower, i.e., 100 ppm. Then, the interaction effect of SDS with four different kinds of PAM (cationic, anionic, zwitterion, and nonionic) on drag reduction has been investigated, respectively, to acquire the optimum combination for drag reduction.

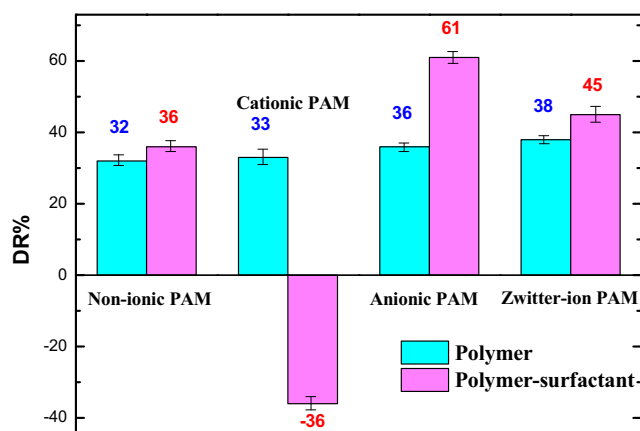


**Fig. 2** Drag reduction of different kinds of PAM (100 ppm) with and without SDS at a certain flow rate under turbulence conditions; the concentration of SDS is 2000 ppm (around CMC)

Figure 2 shows the drag reduction effect of different combinations at a certain flow rate under turbulence conditions; the overall experiment is repeated three times to ensure accuracy, and the error was also shown. As shown in Fig. 2, the combination of nonionic PAM-SDS demonstrates synergetic drag reduction effect. This combination should be favorable for the elongation of the PAM molecular chain owing to the electrostatic repulsion and hydrophobic interaction, just like the previous report [23, 24]. The combination of anionic PAM-SDS and zwitterion PAM-SDS also shows such synergetic effect. On the contrary, the combination of cationic PAM and SDS shows a negative impact on the drag reduction, the coiling, and the collapse of polymer macromolecules which resulted from electrostatic attraction which is supposed to account for this result [13, 23]. Particularly, the combination of anionic PAM and SDS shows superior drag reduction performance than others. Then, the interaction of anionic PAM and SDS with different concentration was investigated further, as well as its effect on drag reduction behavior.

### Interaction of SDS and anionic PAM

#### Surface tension

Surface tension can be used to find the CAC, PSP, and point of free micelle formation. Thus, surface tension measurements were conducted over the PAM/SDS mixtures and compared to that of pure SDS. Here, the PAM concentration was kept constant at 100 ppm, while the SDS concentration varied from 250 to 5000 ppm. The results are presented below in Fig. 3.

As can be seen from Fig. 3, PAM is not a surface-active polymer because the surface tension cannot be reduced further more when PAM was added [28]. We can also conclude that the CMC of SDS is around 2000 ppm, and the CAC and PSP with PAM is about 1750 ppm and 3000 ppm, respectively, from the results of surface tension.

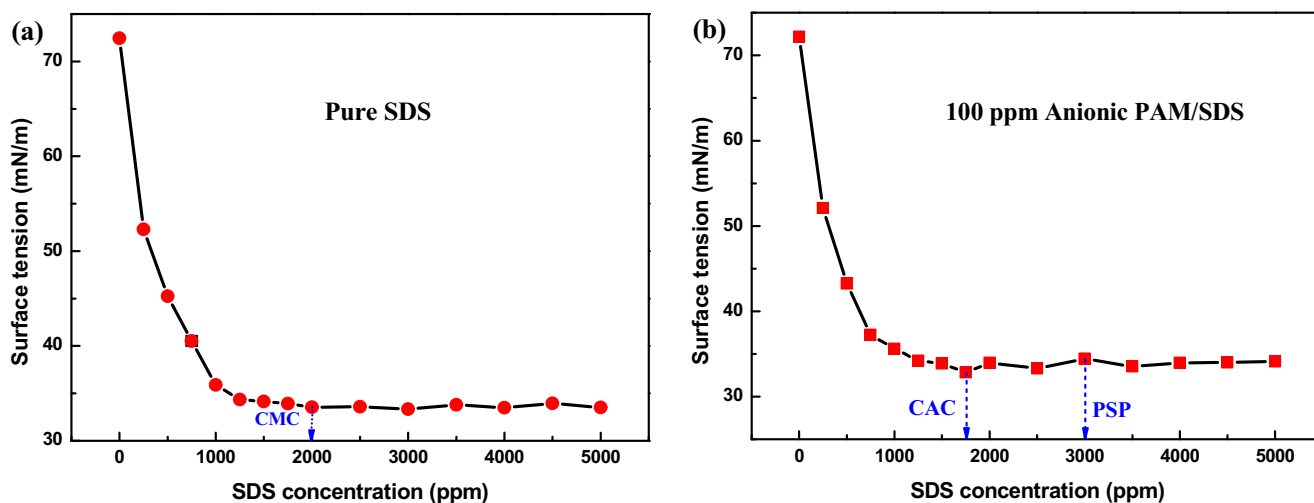


**Fig. 3** Surface tension of SDS solution as a function of SDS concentration with and without anionic PAM (the PAM concentration was kept constant at 100 ppm)

### Conductivity

The CAC and PSP can also be detected through electrical conductivity measurements. Figure 4 shows the typical conductivity plots for pure SDS and mixed 100-ppm anionic PAM and SDS system. For pure SDS solution, conductivity increases with the increase in SDS concentration, then the slope of conductivity plot decreases when the SDS concentration passes by CMC (2000 ppm) due to decreased mobility of the bulky micelles over the highly mobile surfactant molecules.

When 100 ppm anionic PAM is present in the SDS solution, a change in the slope begins at the CAC (1750 ppm). If the conductivity line with the SDS concentration of SDS between 1750 ppm and 2000 ppm for 100 ppm anionic PAM/

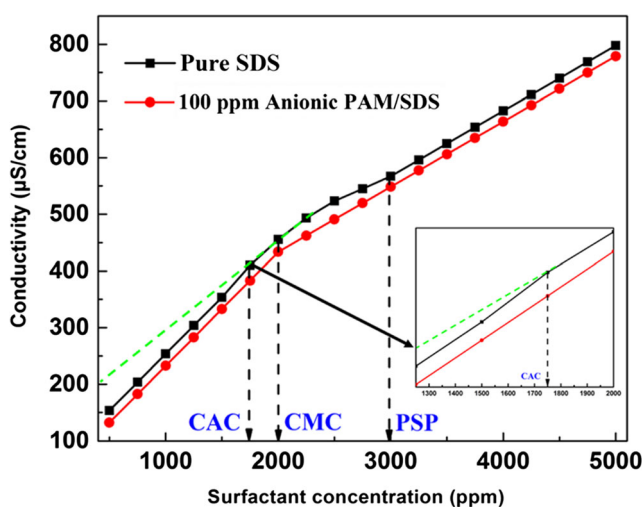


**Fig. 4** Conductivity of the SDS solution as a function of SDS concentration with and without anionic PAM; the green dotted line indicates the transition point where the slope changes for the black curves. (The PAM concentration was kept constant at 100 ppm.)

SDS solution is extended inversely, as also in Fig. 4, we can see that the slope of the green dotted line is a little smaller than that of the original conductivity curve beyond 1750 ppm. To be clearer, the enlarged images for the two conductivity lines are presented in the inset of Fig. 4. We can see a distinct slope change in conductivity for mixed solution at 1750 ppm. The concentration of the surfactant is where surfactant monomers begin to associate with the polymer chains and finish at the PSP (3000 ppm); the polymer molecules are saturated with the surfactant. It is supposed that the conductivity is determined by charge and mobility; when the surfactant molecules begin to form aggregates with the polymer, the slope of conductivity plot will decrease for the lower mobility of the surfactant-polymer aggregate until the polymer molecules are saturated, then maintain a steady increase with the further addition of the surfactant [24]. The CAC and PSP acquired from the conductivity plot are both consistent with that from surface tension results, indicating the reliability of our experimental results.

### Viscosity

Viscosity measurements can be used to detect the conformational changes of polymer chains with the addition of the surfactant. The electrostatic interaction between the oppositely charged polymer and the surfactant is expected to have a strong influence on the viscous behavior of polymer-surfactant solutions [13]. Figure 5 shows the viscosity values for pure SDS and PAM/SDS mixtures, respectively. Again, the PAM concentration was held constant at 100 ppm, while the SDS concentration varied from 0 to 5000 ppm.

For pure SDS solution, the viscosity increases with the increase in SDS concentration, and a sharp increase is achieved around the CMC due to the formation of micelles after which a viscoelasticity fluid is expected [29]. However, for the polymer/surfactant mixture, the change in viscosity

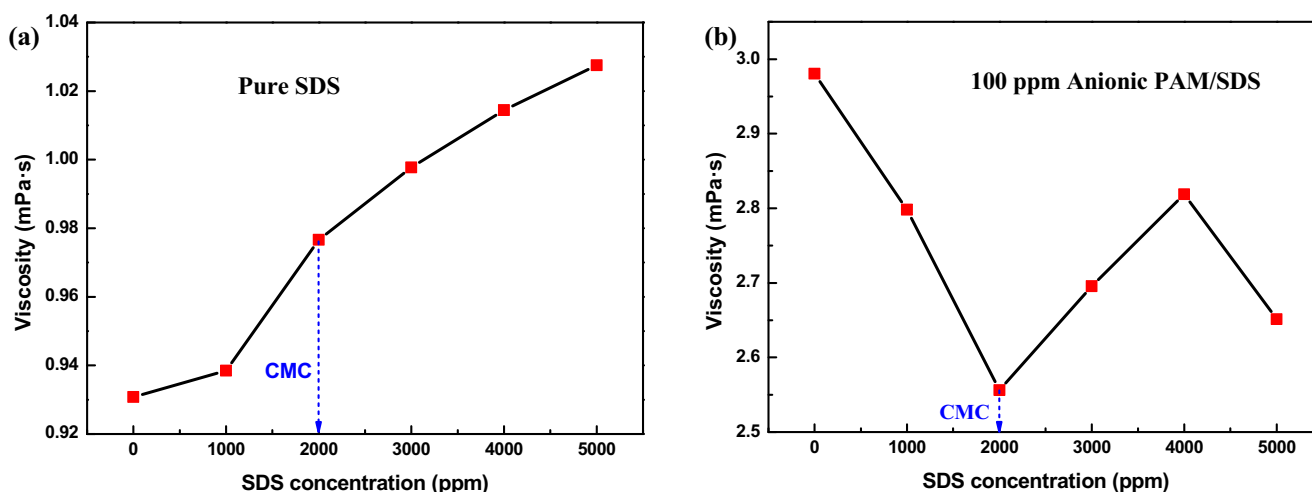


**Fig. 5** Viscosity of SDS solution as a function of SDS concentration with and without anionic PAM (the PAM concentration was kept constant at 100 ppm)

with SDS concentration manifests a complicated trend. The overall trend can be divided into three parts. Firstly, when the concentration of SDS is lower than CMC, there is no micelle formed in the solution. The slight hydrophobic interaction and electrostatic repulsion between a small amount of SDS molecular and PAM molecular chain are supposed to promote the intertangling of PAM molecular and thus the viscosity decreases until the CMC of SDS. When it comes to the second stage, the micelles form with the SDS concentration exceeding CMC, the mixed polymer–surfactant aggregate micelle will form, and the PAM molecule becomes more and more outstretched for the strong interaction of hydrophobic and electrostatic, and then the viscosity increases rapidly. For the third stage, with the concentration of SDS higher than 4000 ppm, the surfactant molecule in the formed mixed micelle increases, and the hydrophobic group will decrease, both of which will weaken the association between polymer molecules and thus lead to the collapse of three-dimensional structures. On the other hand, the stronger electrostatic repulsion will stretch the molecular chain until collapse, then the viscosity of the solution will decrease [30].

### Pipeline flow behavior of solutions

Pure polymer with the mass concentration of 100 ppm and pure surfactant with the concentrations of 1000 ppm, 2000 ppm, 3000 ppm, 4000 ppm, and 5000 ppm, respectively, were tested at different flow rates from 0.2 to 1.3 m<sup>3</sup>/h. Note that here different flow rates correspond to different Reynolds numbers. Then, the mixed solution with the constant polymer 100 ppm and surfactant concentration changing from 1000 to 5000 ppm was tested at the same condition as pure polymer and pure surfactant. The tested results are shown in Fig. 6.

For pure SDS solution (Fig. 6a), the drag reduction effect emerges when the concentration of SDS reaches

4000 ppm. It has been reported that for SDS, when the surfactant solution reaches the CMC (2000 ppm), spherical micelles will be firstly formed in the solution [31]. With the concentration further increased to the transition concentration (CMCII), the spherical micelles in the solution will transform into rod micelles. When the fluid flows, the rod micelles gradually assemble into a shear-inducing structure and a spatial network structure under shear. As a result, the viscosity of the solution increases and becomes a viscoelastic fluid which, in turn, leads to the drag reduction effect [32]. The drag reduction effect begins at a certain Reynolds number, considering that the shear action can also facilitate the formation of micelles. Then, the formation of a more viscoelastic shear-induced structure and spatial network structure will contribute to drag reduction of fluid. Here, we consider that when Re is lower than 15,000, the low shear force is not strong enough to promote the formation of the shear-induced structure, nor drag reduction, though the SDS concentration is already very high. We can also conclude that considerable shear force is necessary for the formation of the shear-induced structure for the surfactant solution which is essential for the drag reduction. Meanwhile, it is assumed that only when there are rod micelles will the drag reduction performance be acquired under a certain flow rate. Here we also can infer that the CMCII is higher than 3000 ppm.

The drag reduction curves of the surfactant solution with the concentration of 4000 ppm and 5000 ppm both show the same trend that the drag reduction effect begins at a certain Reynolds number. However, the surfactant solution with the concentration of 5000 ppm shows a drag reduction effect at a lower Reynolds number and a higher drag reduction rate at the same Reynolds number compared with that of 4000 ppm, which can be contributed to the formation of a more

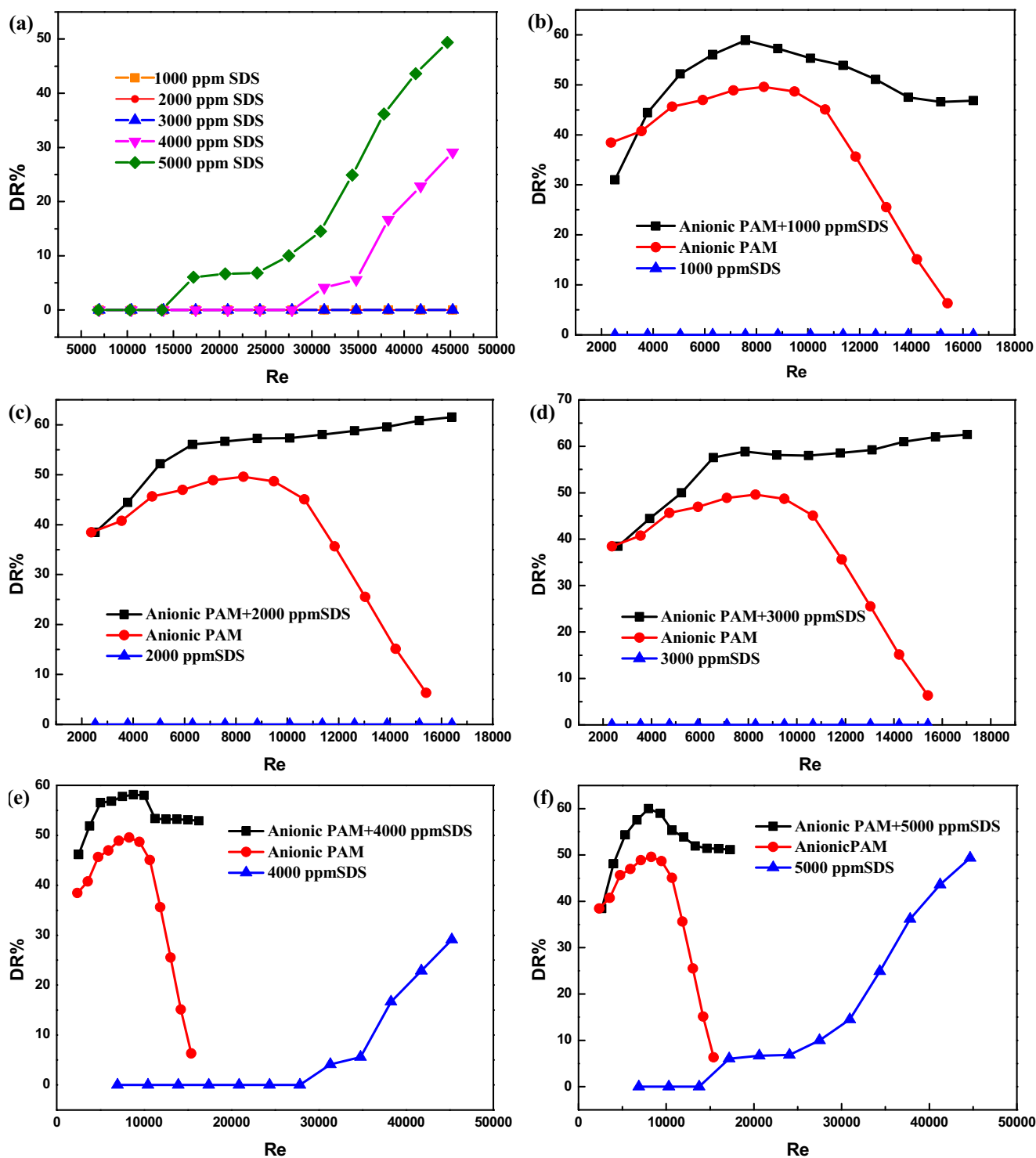


**Fig. 6** Drag reduction curves of mixed solution of 100 ppm anionic PAM and SDS and pure SDS solution at different SDS concentrations (the PAM concentration was kept constant at 100 ppm)

viscoelastic shear-inducing structure and spatial network structure at a higher SDS concentration [12].

For pure PAM solution, the drag reduction effect emerges at a very low Reynolds number beyond 2000, then reaches the maximum degree of drag reduction with the increase in

Reynolds number and begin to decrease with the further increase in Reynolds number owing possibly to the breaking of the polymer molecular chain under high shear rate [33, 34].

The drag reduction curves of five concentrations (1000 ppm, 2000 ppm, 3000 ppm, 4000 ppm, and

5000 ppm) of the mixed solution are shown in Fig. 6b and Fig. 6f, respectively. The results indicate that the curve of the mixed solution is different from that of the pure PAM solution. Firstly, the degree of drag reduction for the mixed solution is higher than that of pure PAM solution in the entire range of flow. Secondly, the mixed solution retains the drag reduction performance at a higher Reynolds number while the PAM solution gradually loses drag reduction ability with the increase in the Reynolds number. Thirdly, the mixed solution of different SDS concentration exhibits a different drag reduction behavior. The best drag reduction effect for the onset Reynolds number (the Reynolds number at which drag reduction performance begins to emerge) is achieved at the concentration of 4000 ppm, while the best drag reduction effect for a higher Reynolds number is achieved at the concentration of 3000 ppm. Meanwhile, the mixed solution with SDS concentration of 2000 ppm (CMC) and 3000 ppm (PSP) shows a rising trend with the increase in the Reynolds number in our tested range (as shown in Fig. 6c and Fig. 6d), and the better drag reduction performance is presented for 3000 ppm. But the mixed solution with SDS concentrations of 1000 ppm, 4000 ppm, and 5000 ppm shows an opposite trend with the further increase in the Reynolds number in our tested range (as shown in Fig. 6b, Fig. 6e, and Fig. 6f). We have indeed tried to further increase the flow rate to study the drag reduction performance of the PAM+SDS solution under  $Re$  higher than 20,000. However, our screw pump cannot steadily work under such higher  $Re$  working conditions. As a result, there is no experimental data when  $Re$  is larger than 20,000 for PAM and PAM+SDS solutions.

The diversity of the drag reduction performance is more evident at a higher Reynolds number. To present the drag reduction phenomenon under a higher shear rate in our experiment evidently, the drag reduction data of the mixed solution

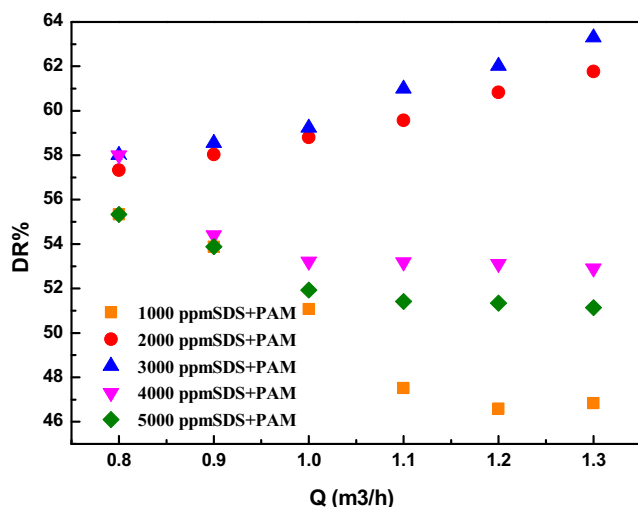


**Fig. 7** Drag reduction behavior of the mixed solution at a high flow rate higher than  $0.8 \text{ m}^3/\text{h}$

with different SDS concentration at high flow rates (higher than  $0.8 \text{ m}^3/\text{h}$ ) are shown in Fig. 7.

The morphology of the mixed solution with 3000 ppm SDS and 100 ppm anionic PAM is presented in Fig. 8c, and the morphology of pure 100 ppm anionic PAM solution and 3000 ppm SDS solution is also presented in Fig. 8a, b, respectively, for comparison. We can see the network-like structure which is different from Fig. 8a, b, clearly from Fig. 8c, and it is consistent with what we analyzed above.

To verify the hydrophobic interaction and electrostatic repulsion between PAM and SDS molecular furthermore, FTIR spectra for 100 ppm anionic PAM solution, 3000 ppm SDS solution, and their mixture are shown in Fig. 9. We can hardly see any difference between pure SDS solution and PAM/SDS mixture. As shown in Fig. 9, the peak at  $1638$  and  $3449 \text{ cm}^{-1}$  was assigned to the vibrational absorption of the O–H bond from solvent water. The strong peak at  $2062 \text{ cm}^{-1}$  belongs to the C–H bond of the alkyl chain, while the peaks in the range from  $1000$  to  $1100 \text{ cm}^{-1}$  were due to the vibrations of the S=O bond of the sulfate group in the SDS molecule, and the peak at  $1250 \text{ cm}^{-1}$  can be ascribed to the C–O–S unit. What was mentioned above is similar to the literature [35]. It should be noted that because of the lower density of PAM, the intensity of FTIR spectra is slighter, which will not be analyzed in detail here. Thus, it can be inferred that there is not any new chemical group formed in the mixture, neither any change in molecular groups. It is the network that resulted from hydrophobic interaction and electrostatic repulsion between PAM and SDS molecule that promotes drag reduction effect.

## Mechanism discussion

We can see clearly from Fig. 7 that the mixed solution with 2000 ppm and 3000 ppm SDS shows a better drag reduction behavior, especially the latter. The probable illustration of the interaction of PAM with different SDS concentrations under lower shear rate (with the flow rates lower than  $0.8 \text{ m}^3/\text{h}$ ) is shown schematically in Fig. 10. It should be helpful to predict and analyze the change in the formation if the shear rate undergoes further increase. Figure 10a presents the coiled PAM molecular chains under slight interaction of the PAM molecule with SDS at the concentration of 1000 ppm. Figure 10b presents the interaction of 2000 ppm SDS with PAM in the lower flow rate vividly, and Fig. 10c represents the case for 3000 ppm SDS. When the concentration of SDS reaches 2000 ppm (CMC), micelles begin to form, and the large amount of a single surfactant molecule and new formed surfactant micelle interacts with the PAM molecule through a slight hydrophobic interaction and electrostatic repulsion, promoting the coil of the PAM molecule.

With the increase in shear rate, the coiled PAM molecular chain gradually stretches under the action of shear force.



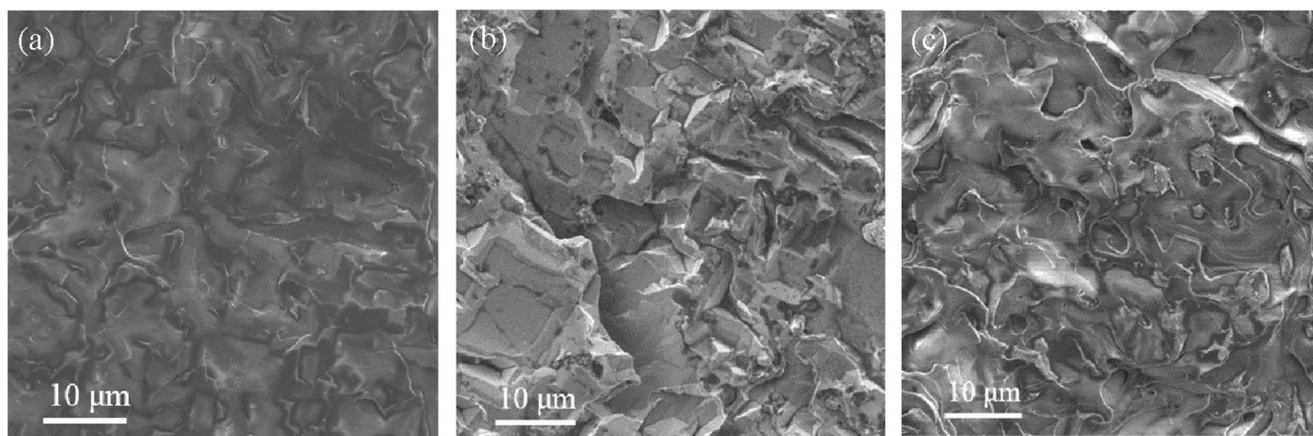


**Fig. 8** The SEM image of **a** 3000 ppm SDS solution, **b** 100 ppm anionic PAM solution, and **c** mixed solution with 3000 ppm SDS and 100 ppm anionic PAM

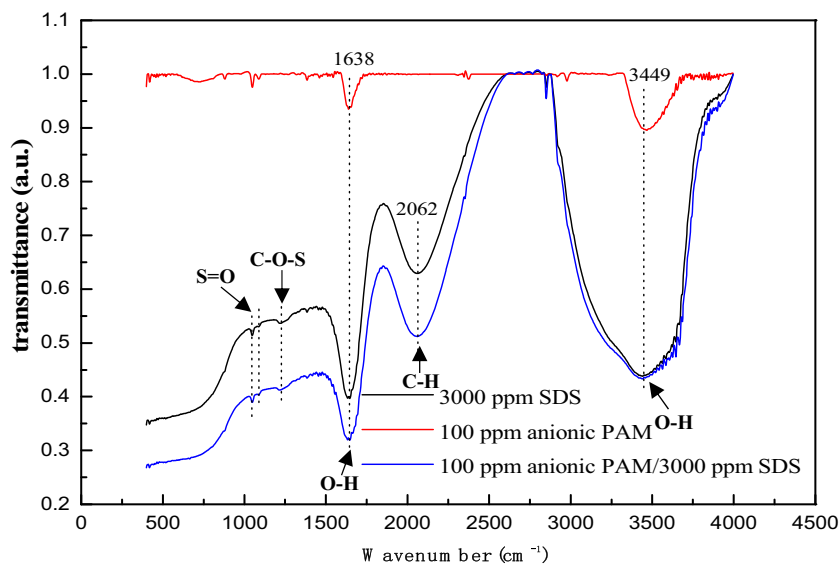
Then, a network structure will form with new formed surfactant micelles. Here, the surfactant in the node of the polymer molecular chain is expected to prevent the molecular chain from breaking under high shear rates. With the concentration of SDS increasing to 3000 ppm (PSP), an interaction between surfactant and PAM becomes stronger under dual action of hydrophobic interaction and electrostatic repulsion for the formation of large amounts of micelles. Micelles present on the backbone of PAM chains can cause the expansion of the polymer chains as the chains extend, SDS micelles contribute to protecting polymer chains from shear stress to some extent, then the %DR and resistance to shear degradation can be improved [21].

It appears that the addition of 1000 ppm causes a slight interaction with the polymer, and the small amount of surfactant is not enough to form micelles on the backbone of polymer molecules (Fig. 8a). The PAM molecular chain cannot expand enough under shear to improve the drag reduction behavior, nor the resistance of polymer chains against

mechanical degradation. Therefore, the drag reduction effect of mixed solution with 1000 ppm SDS is weaker [23].

The mixed solution with SDS concentrations of 4000 ppm and 5000 ppm shows a similar drag reduction behavior during pipe flow experiment, both demonstrating a higher drag reduction rate at a lower flow rate, but decreasing rapidly with the increase in flow rate. When the concentration of SDS reaches 4000 ppm, rod-like or worm-like micelles will form (which can be verified from the pure drag reduction experiment presented above as in Fig. 6a), the strong interaction of large amounts of rod-like micelles with polymer chain facilitates the formation of a three-dimensional network (Fig. 8d), and thus the viscosity reached the maximum value (as shown in Fig. 5); with the increase in shear rate, the polymer chain becomes more and more outstretched for the strong hydrophobic interaction and electrostatic repulsion. The outstretched polymer chain will have a better drag reduction performance, but weaker elasticity. When the shear rate increases further, the polymer chain with lower elasticity is

**Fig. 9** The FTIR spectra of 3000 ppm SDS solution, 100 ppm anionic PAM solution, and mixed solution with 3000 ppm SDS and 100 ppm anionic PAM



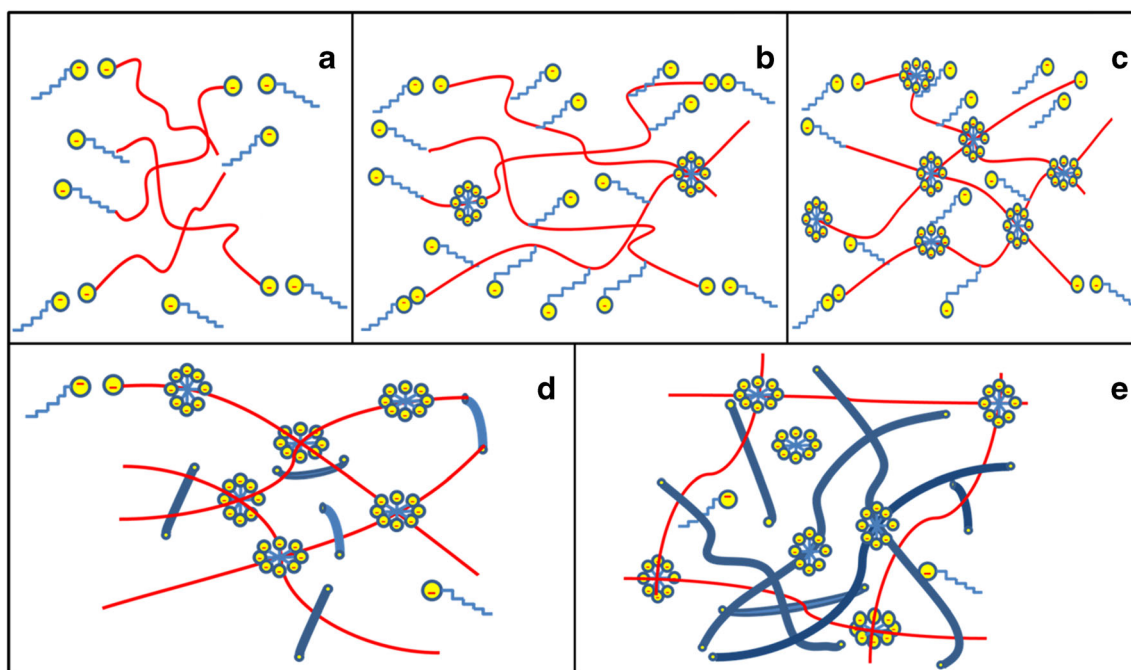


**Fig. 10** Illustration of the interaction of PAM with SDS of different concentrations under lower shear rate (with the flow rates lower than  $0.8 \text{ m}^3/\text{h}$ ). **a, b, c, d,** and **e** are for 1000 ppm, 2000 ppm, 3000 ppm, 4000 ppm, and 5000 ppm, respectively

liable to breakdown, then the degree of drag reduction will decrease rapidly [36]. For the mixed solution with 5000 ppm SDS, the hydrophobic interaction and electrostatic repulsion are stronger than that of 4000 ppm. Therefore, the polymer chain is more outstretched and less elastic (almost become linear) under a lower flow rate (Fig. 8e). It can even be inferred that the molecular chain has been broken partially from the lower-viscosity value mentioned above. Thus, the mixed solution with 5000 ppm SDS will be broken more easily when subjected to a higher shear rate.

## Conclusion

In this study, we firstly selected the optimum combination of anionic surfactant SDS and PAM. Then the intensification of drag reduction performance caused by mixtures of anionic surfactant and anionic PAM solutions was investigated, and the surface tension and viscosity were performed to explain the interaction of SDS and anionic PAM complementally. Our work should be of value for the drag reduction in the application such as shale gas fracturing and various fluid transports. The main outcomes of our study are summarized as below:

- 1) Preferable drag reduction performance was achieved by the combination of anionic surfactant and anionic PAM under certain conditions for the stronger hydrophobic interaction and electrostatic repulsion caused by the same charge.

- 2) Drag reduction performance acquired from the combination of anionic surfactant and anionic PAM is better than either of the single additive in our whole pipe experiment, especially under a high shear rate.
- 3) The degree of drag reduction is strongly dependent on the concentration of SDS, and more influential in the high Reynolds number range. The best drag reduction performance is obtained for the SDS concentration around PSP (3000 ppm), for the micelles present on the backbone of PAM chains which can cause the polymer chains to expand and help protect polymer chains from shear stress.
- 4) When the concentration of SDS exceeds PSP, the more outstretched and less elastic polymer chain will form under the stronger hydrophobic interaction and electrostatic repulsion, which are liable to breakdown when subjected to a high shear rate, thus resulting in a weaker drag reduction performance in high flow rate.

**Funding information** This study was financial supported by the National Natural Science Foundation of China (No. 51776165, 51888103) and Shanxi Science & Technology Co-ordination & Innovation Project (Contract No. 2017ZDXM-GY-067). This work was also supported by the China Fundamental Research Funds for the Central Universities.

## Compliance with ethical standards

**Conflict of interest** The authors declare that they have no conflict of interest.

## References

- Virk PS (1975) Drag reduction fundamentals. *AICHE J* 21(4):625–656
- Lumley JL Drag reduction in turbulent flow by polymer additives. *J Polym Sci Part A: Polym Chem* 7.1(2010)
- Ohlendorf D, Interthal W, Hoffmann H (1986) Surfactant systems for drag reduction: physico-chemical properties and rheological behaviour. *Rheol Acta* 25(5):468–486
- Lucas EF, Mansur CRE, Spinelli L, Queirós YGC (2009) Polymer science applied to petroleum production. *Pure Appl Chem* 81(3):473–494
- Yoon H, Sik HHC (2006) Drag reduction in turbulent channel flow with periodically arrayed heating and cooling strips. *Phys Fluids* 18(2):1093
- Harwigsson I, Hellsten M (1996) Environmentally acceptable drag-reducing surfactants for district heating and cooling. *J Am Oil Chem Soc* 73(7):921–928
- Obry M (1980) Polymer drag reduction in large pipes and sewers: results of recent field trials. *J Rheol* 24(5):667–684
- Figueredo RCR, Sabadini E (2003) Firefighting foam stability: the effect of the drag reducer poly (ethylene) oxide. *Colloids Surf A Physicochem Eng Asp* 215 1:77–86
- Abubakar A (2014) Roles of drag reducing polymers in single- and multi-phase flows. *Chem Eng Res Des* 92(11):2153–2181
- Rouse PE, Sittel K (1953) Viscoelastic properties of dilute polymer solutions. *J Appl Phys* 24(6):690–696
- Yoshizaki H (1989) Ultrasonic viscoelasticity and excess absorption in polymer solution. *Polym J* 21(11):905–913
- Jinjia W, Chonghai H, Na XU (2016) Research progress concerning turbulent drag reduction of surfactant solution. *Chem Ind & Eng Pro (China)*
- Mohsenipour AA, Pal R, Prajapati K (2013) Effect of cationic surfactant addition on the drag reduction behaviour of anionic polymer solutions. *Can J Chem Eng* 91(1):181
- Dongjie L et al (2018) Molecular dynamics simulation of self-assembly and viscosity behavior of PAM and CTAC in salt-added solutions. *J Mol Liq* 268:131–139
- Mohsenipour A, Asghar R (2013) Drag reduction in turbulent pipeline flow of mixed nonionic polymer and cationic surfactant systems. *Can J Chem Eng* 91(1):190–201
- Anthony O, Zana R (1996) Interactions between water-soluble polymers and surfactants: effect of the polymer hydrophobicity. 1. Hydrophilic polyelectrolytes. *Langmuir*. 12(8):1967–1975
- Thuresson K (1995) Effect of surfactant on structural and thermodynamic properties of aqueous solutions of hydrophobically modified ethyl (hydroxyethyl) cellulose. *Langmuir* 11(10):3730–3736
- Deo P et al (2007) Interactions of a hydrophobically modified polymer with oppositely charged surfactants. *Langmuir*. 23(11):5906–5913
- Deo P (2003) Interactions of hydrophobically modified polyelectrolytes with surfactants of the same charge. *Langmuir*. 19(26):10747–10752
- Parathakkatt S, George J, Sankarakutty SM, Sreejith L (2009) Polymer induced structures in cetylpyridinium chloride–octanol micellar system. *J Polym Res* 16(5):577–582
- Liu D, Wang Q, Wei J (2018) Experimental study on drag reduction performance of mixed polymer and surfactant solutions. *Chem Eng Res Des*
- Malcher T, Gzylmalcher B (2012) Influence of polymer-surfactant aggregates on fluid flow. *Bioelectrochemistry* 87 10:42–49
- Mohsenipour AA, Pal R (2013) The role of surfactants in mechanical degradation of drag-reducing polymers. *Bioelectrochemistry* 52(3):1291–1302
- Mohsenipour AA, Pal R (2013) Synergistic effects of anionic surfactant and nonionic polymer additives on drag reduction. *Chem Eng Commun* 200(7):24
- Nagarajan R (1980) Thermodynamics of surfactant-polymer interactions in dilute aqueous solutions. *Chem Phys Lett* 76(2):282–286
- Ruckenstein E, Huber G, Hoffmann H (1987) Surfactant aggregation in the presence of polymers. *Langmuir*. 3(3):382–387
- Monteux C (2007) Determining the mechanical response of particle-laden fluid interfaces using surface pressure isotherms and bulk pressure measurements of droplets. *Phys Chem Chem Phys* 9(48):6344–6350
- Goddard ED (2002) Polymer/surfactant interaction: interfacial aspects. *J Colloid Interface Sci* 256(1):228–235
- YU B (2004) Numerical and experimental investigation of turbulent characteristics in a drag-reducing flow with surfactant additives. *Int J Heat Fluid Flow* 25(6):961–974
- Biggs S, Selb J, Candau F (1992) Effect of surfactant on the solution properties of hydrophobically modified polyacrylamide. *Langmuir*. 8(3):838–847
- Li FC (2008) Experimental study of drag-reduction mechanism for a dilute surfactant solution flow. *Int J Heat Mass Tranf* 51(3):835–843
- Lin Z (2016) Comparison of the effects of methyl- and chloro-substituted salicylate counterions on drag reduction and rheological behavior and micellar formation of a cationic surfactant. *Rheol Acta* 55(2):117–123
- Sher I, Hetsroni G (2008) A mechanistic model of turbulent drag reduction by additives. *Chem Eng Sci* 63(7):1771–1778
- Liberatore MW (2004) Turbulent drag reduction of polyacrylamide solutions: effect of degradation on molecular weight distribution. *J Non-Newton Fluid* 123(2–3):175–183
- Krstonošić V, Milanović M, Dokić L (2019) Application of different techniques in the determination of xanthan gum-SDS and xanthan gum-tween 80 interaction. *Food Hydrocoll* 87:108–118
- Liu Z-y (2017) Impact of the microstructure of polymer drag reducer on slick-water fracturing. *Geofluids*. 2017:1–8

**Publisher's note** Springer Nature remains neutral with regard to jurisdictional claims in published maps and institutional affiliations.